Unraveling the Origin of Low Optical Efficiency for Quantum Dot White Light-Emitting Diodes From the Perspective of Aggregation-Induced Scattering Effect

Zong-Tao Li, *Member, IEEE*, Jie-Xin Li, Zi-Hao Deng, Jia-Yong Liang, and Jia-Sheng Li

***Abstract*— Quantum dots (QDs) are promising materials for various optoelectronic applications. However, the efficiency of QD white light-emitting diodes (QD-white-LEDs) is not at the desired level, particularly when the QD concentration in the silicone matrix is high and the corresponding mechanism has not been fully elucidated. In this study, we experimentally and theoretically investigated the aggregation-induced scattering (AIS) effect of QDs in silicone and unraveled the origin of low efficiency for QD-white-LED devices. Three-dimensional finite-difference time domain and ray tracing simulations were carried out to establish the AIS model for QDs. Results indicate that the AIS effect is stronger for higher QD concentrations and leads to a larger effective aggregate size (EAS), which was confirmed by comparing with the experimental results of QD-silicone films. Furthermore, we found that the AIS effect causes a significant reduction in the radiant efficiencies of QD-white-LEDs when the EAS exceeds 50 particles, which is validated by fabricated devices. According to the spectral energy analysis, the low efficiency of QD-white-LEDs can be attributed to a strong AIS effect at high QD concentrations, causing severe backscattering and reabsorption loss. This study is also important for nondestructive testing the degree of aggregation demonstrated by QDs in a silicone matrix and for precisely modeling QD-white-LEDs.**

***Index Terms*— Aggregation-induced scattering (AIS), optical efficiency, precise modeling, quantum dots (QDs).**

Manuscript received January 30, 2021; revised February 15, 2021; accepted February 16, 2021. Date of publication March 9, 2021; date of current version March 24, 2021. This work was supported in part by the Science and Technology Program of Guangdong Province under Grant 2020B0101030008; in part by the National Natural Science Foundation of China under Grant 51775199 and Grant 51735004; and in part by the Fundamental Research Funds for the Central Universities. The review of this article was arranged by Editor C. Bayram. *(Corresponding author: Jia-Sheng Li.)*

Zong-Tao Li is with the National and Local Joint Engineering Research Center of Semiconductor Display and Optical Communication Devices, South China University of Technology, Guangzhou 510641, China, and also with the Guangdong Provincial Key Laboratory of Semiconductor Micro Display, Foshan Nationstar Optoelectronics Company Ltd., Foshan 528000, China.

Jie-Xin Li, Zi-Hao Deng, Jia-Yong Liang, and Jia-Sheng Li are with the National and Local Joint Engineering Research Center of Semiconductor Display and Optical Communication Devices, South China University of Technology, Guangzhou 510641, China (e-mail: jiasli@foxmail.com).

Color versions of one or more figures in this article are available at https://doi.org/10.1109/TED.2021.3060698.

Digital Object Identifier 10.1109/TED.2021.3060698

I. Introduction

QUANTUM dots (QDs) have attracted great attention in recent years because of their important practical applications. Owing to their excellent properties such as high photoluminescence quantum yield (PLQY), narrow emission spectra, and ease of manufacturing [1], [2], they have emerged as one of the most promising materials for color conversion [3]. These advantages have inspired extensive research on QDs, which has resulted in numerous photoelectric applications in various fields, such as solar cells [4], [5], detectors [6], [7], and in particular, light-emitting diodes (LEDs) [8]–[10]. However, the efficiency of QD-white-LEDs obtained so far is not at the desired levels. This is mainly because of the host material effect and reabsorption [11], [12], which makes their efficiency much lower than that of LEDs based on traditional phosphor composites [13], [14].

In general, QDs are dispersed into a transparent silicone matrix to form QD-silicone composites, which further prevents the oxidation of QDs [15]. Such QD-silicone composites have been utilized as color converters in solid-state lighting sources such as LEDs to control their chromatic properties [16], [17]; for example, blue light emitted from LED chips can be converted into light of other colors. However, this method is often plagued by problems such as aggregation-induced quenching (AIQ) [18] during matrix exchange. For instance, the PLQY of liquid QDs has been found to be over 90% [1], [19], however, that of QDs in silicone drops sharply from the synthesis batch in the liquid state to the host matrix in the solid state [20]. Moreover, QDs generally exhibit a strong absorption of their emitted light, which is comparable with the excitation blue light from LED chips, leading to serious reabsorption loss [21]. In particular, the efficiency of QD-white-LEDs is extraordinarily low at high QD concentrations [22], and corresponding mechanism has not been fully elucidated. Most previous studies believe that the scattering effect of QDs on the device efficiency can be neglected owing to their small size, which is only a few nanometers [23]. The underlying mechanisms for low efficiency are mainly attributed to reabsorption and AIQ losses at high QD concentrations, which substantially reduce the color conversion efficiency of these devices [24]. Recently, our previous study introduced QD/SBA-15 nanocomposite

particles to solve the resorption issue and demonstrated a mechanism to suppress QD light propagating pores, achieving a record luminous efficacy of 206.8 lm W^{-1} at 20 mA for white LED integrating only green QDs [25]. However, there is a significant gap in the current literature with respect to the aggregation-induced scattering (AIS) effect of QDs in a silicone matrix, which can have a potential impact on the optical performance of QD-white-LEDs owing to an increase in the effective size of the particle because of aggregation.

In this study, we experimentally and theoretically investigated the AIS effect of QDs in silicone and unraveled the origin of low efficiency for QD-white-LED devices. The AIS effect on the optical behavior of QDs in silicone was investigated and 3-D finite-difference time domain (FDTD) and ray tracing (RT) simulations were combined to establish the AIS model. Furthermore, the AIS effect on the efficiency of LED devices can be obtained, unraveling the origin of low optical efficiency for QD-white-LED. According to the spectral energy analysis, it is confirmed that a strong AIS effect at high QD concentration leads to severe backscattering and reabsorption loss, which further result in a low efficiency. Moreover, this study is also important for nondestructive testing the degree of aggregation demonstrated by QDs in a silicone matrix and for precisely modeling QD-white-LEDs.

II. Experimental

The green CdSe/ZnS QDs used in this study were purchased from Beijing Beida Jubang Science and Technology Co., Ltd., China. Their peak emission wavelength is 525 nm and their PLQY is approximately 85%. The blue LED devices without a silicone encapsulant were purchased from Foshan NationStar Optoelectronics Co., Ltd., China, which have a peak emission wavelength at 455 nm; polydimethylsiloxane (PDMS) was used as the silicone encapsulant. The dispersion matrix for the QDs was purchased from Dow Corning, USA, whereas the hexane used as the solvent for QD dispersion was purchased from Aladdin Reagents, China.

Previous studies on QD-white-LED generally disperse QDs into a silicone matrix through the solvent evaporation method [1], [13], [15], [25]. For investigating the distribution of QDs in a more general encapsulant application of LED devices, the same preparation process is used to fabricate the films and devices. First, varying amounts of CdSe-based QDs were completely dissolved in a 3-mL hexane solution and mixed with 1 g of PDMS. Subsequently, the hexane-silicone-QD mixture was evaporated at 50 °C to completely volatilize the hexane and obtain the QD-slurry. Next, this slurry was injected into a stainless steel mold and moved to an oven, preset at a temperature of 90 °C, for 1 h to cure the silicone. Finally, the films having a thickness of 0.5 mm and different QD concentrations were obtained. As for the LED devices, the QD-slurry was obtained using the same procedure, which was then injected into blue LED devices to complete the fabrication process. The silicone matrix was cured for 2 h at a temperature of 60 °C to avoid the optical degradation of the QDs. Six different samples of the LED devices were used for each case in the experiments.

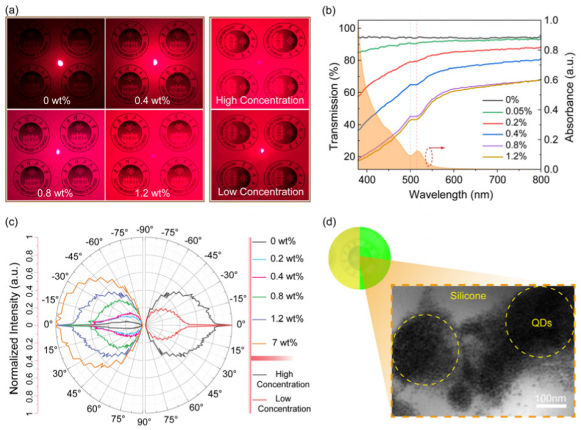

Fig. 1. (a) Transmitted laser spots in QD-silicone composites with different QD concentrations (left and middle columns) and with different QD concentrations but having an equivalent amount of QDs (rightmost column). (b) Transmission spectra of QD-silicone composites with different concentrations and the absorption spectrum of QDs. (c) NTIDs of QD-silicone composites with different QD concentrations (left) and with different QD concentrations but having an equivalent amount of QDs (right). (d) Photograph of a QD-silicone composite with a QD concentration of 0.8 wt% under visible light (left) and UV-light (right). The inset shows the TEM image of a frozen section of the QD-silicone composite obtained using the freeze ultrathin sectioning method, demonstrating how the QDs are distributed in the silicone matrix.

Frozen sections of the films were prepared using an ultramicrotome from Leica, Germany. The distribution of QDs in the silicone matrix was observed using a transmission electron microscopy (TEM) instrument from JEOL Ltd., Japan. The absorbance of the QDs was measured using an UV–vis spectrometer from Shimadzu Corporation, Japan. The optical performance of the LEDs was measured using an integrating sphere system from Instrument Systems GmbH, Germany, and the injection current was provided by a power source from Keithley Instruments, USA.

III. Results and Discussion

A. AIS Effect of QDs in Silicone

Owing to the instability of QDs caused by oxidation in air, it is essential to incorporate QDs into an encapsulant matrix, generally dispersing QDs into a transparent silicone matrix to form QD-silicone composites. Herein, we conducted experiments to validate the AIS effect on the optical behavior of QDs in silicone (QD-silicone composite). The QD concentrations were set according to the most common concentration in the LED package manufacturing processes [13], [14], [26], ranging from 0 to 1.2 wt%. In general, QDs first absorb the incident light and then emit a light that is optically isotropic, thereby enhancing the transmitted laser spot. In our experiments, we used a red laser source with a central wavelength of 625 nm and green QDs. This is because green QDs have near-zero absorbance at 625 nm, and, hence, it can be ensured that there are almost no color conversion events when using this radiation source. Hence, the impact caused by the light emitted by QDs can be neglected for better studying the scattering behavior of QDs in silicone.

Fig. 1(a) shows the transmitted laser spots in QD-silicone composites having different QD concentrations. We observe

that the laser spot becomes weaker as the QD concentration increases and almost disappears when the concentration is sufficiently high. The reduction in transmittance of the laser spot displayed by the different QD-silicone composites is quite noticeable, which implies that the scattering of light increases with increasing QD concentration. To further prove this hypothesis, we obtained the transmission spectra of these QD-silicone composites using a fluorescence photometer, which are presented in Fig. 1(b). It is observed that the transmittance of the QD-silicone composites decreases as the QD concentration increases. We see that there is a strong absorption of the incident light by the QDs for wavelengths below 600 nm. This corresponds to a decrease in the transmittance of the composite with increasing QD concentration, which is attributed to an enhanced color conversion. Moreover, there is a peak in the absorption spectrum of the QDs at a wavelength of ∼520 nm that directly corresponds to a dip in the transmission spectra of the QD-silicone composites, which substantiates the above claim.

However, the absorbance is almost zero for wavelengths above 600 nm, which in turn indicates that the drop in transmittance is not related to color conversion events. In addition, the refractive index of the QD-silicone composites remains almost constant as the QD concentration is increased from 0 to 1.2 wt%, indicating that the refractive index is independent of the QD concentration. Therefore, the decrease in transmittance of the QD-silicone composites can instead be attributed to an increase in backscattering caused by the QDs, which results in more reflected light at the expense of transmitted light.

Furthermore, we measured the transmission intensity distributions of the QD-silicone composites using a laser platform (also having a wavelength of 625 nm) that can be found elsewhere [27], [28]. To better elucidate the scattering effect of QDs in silicone, the intensity data were processed by a logarithmic operator to obtain the corresponding normalized transmission intensity distributions (NTIDs), which are shown in Fig. 1(c). Note that the radiation from the laser source was incident perpendicular to the composite surface to avoid refraction. We observe that the scattering effect of the QD-silicone composites on the incident light becomes stronger as the QD concentration increases. The transmission intensity is mostly concentrated along the laser incident direction (i.e., 0° direction) at relatively low QD concentrations; however, the NTID becomes more isotropic when the QD concentration is sufficiently high. Therefore, these results demonstrate that the scattering in QD-silicone composites becomes more pronounced at higher QD concentrations. In general, the scattering effect in composites is enhanced as the number of nanoparticles increases; however, the scattering caused by QDs is generally considered to be negligible according to the Rayleigh scattering theory [29] owing to their very small size (usually below 10 nm). Thus, although the number of nanoparticles in the QD-silicone composites increases with concentration, their scattering ability is still insufficient to have a significant impact on the optical performance of the device.

To demonstrate that the scattering effect observed in QD-silicone composites [see e.g., Fig. 1(c)] is not simply owing to the number of QDs, two kinds of QD-silicone composites were fabricated having an equivalent number of QDs. The high-concentration QD-silicone composite has a QD concentration of 1.2 wt% and a thickness of 0.5 mm. whereas the low-concentration QD-silicone composite has a QD concentration of 0.05 wt% and a thickness of 12 mm to ensure the coincidence of nanoparticles in the light propagation regions. The radiation from the laser source was again incident perpendicular to both the composites. The rightmost column of Fig. 1(a) shows the transmitted laser spots in these two composites. We observe that the laser spot in the high-concentration QD-silicone composite is weaker than that in the low-concentration composite despite having an equivalent number of QDs. This implies the presence of a stronger scattering effect in the high-concentration composite, which is further supported by the corresponding NTID shown in Fig. 1(c). These results can be attributed to the generation of a large aggregation of particles at a high QD concentration, which gives rise to a strong AIS effect on visible light.

To validate this viewpoint, we obtained frozen sections of QD-silicone composites with a QD concentration of 0.8 wt% using the freeze ultrathin sectioning method; subsequently, TEM was used to observe the QD distribution in silicone. We observe from Fig. 1(d) that the QDs aggregate to form large particles instead of being uniformly dispersed in the silicone matrix. The size of these QD-aggregates can reach up to hundreds of nanometers for a QD concentration of 0.8 wt%. This in turn implies that the strong scattering effect observed in QD-silicone composites with high QD concentrations is owing to the generation of a large aggregation of particles. In the next section, we will expand upon this hypothesis and confirm it by establishing the AIS model.

B. AIS Model of QDs in Silicone

To obtain the AIS model for QDs having various aggregate sizes, we employed the 3-D FDTD method using the commercial software Lumerical FDTD Solution. Fig. 2(a) shows a schematic of the mono-dispersion and aggregate-dispersion systems, which were used to uniformly disperse single QDs and QD-aggregates in the silicone matrix, respectively. For simplicity, the QD-aggregates were created using the densest sphere packing. These idealized mono-dispersion and aggregate-dispersion systems were used to establish the AIS model. In our simulations, the FDTD method was used to solve Maxwell's curl equations based on the Yee cell [30]. The detailed FDTD setups for the mono-dispersion and aggregate-dispersion systems are illustrated in Fig. 2(b). A perfectly matched layer (PML) was used as the boundary condition, which surrounds the FDTD computational region to absorb the escaping light. To divide the simulation region into a total-field and a scattered-field region, a total-field scattered-field (TFSF) source with a central wavelength of 625 nm was used, which surrounds the dispersion systems. A transmission-monitor (T-monitor) box consisting of a series of plane monitors was used to record the electromagnetic field passing through them, whereas electromagnetic field detectors were

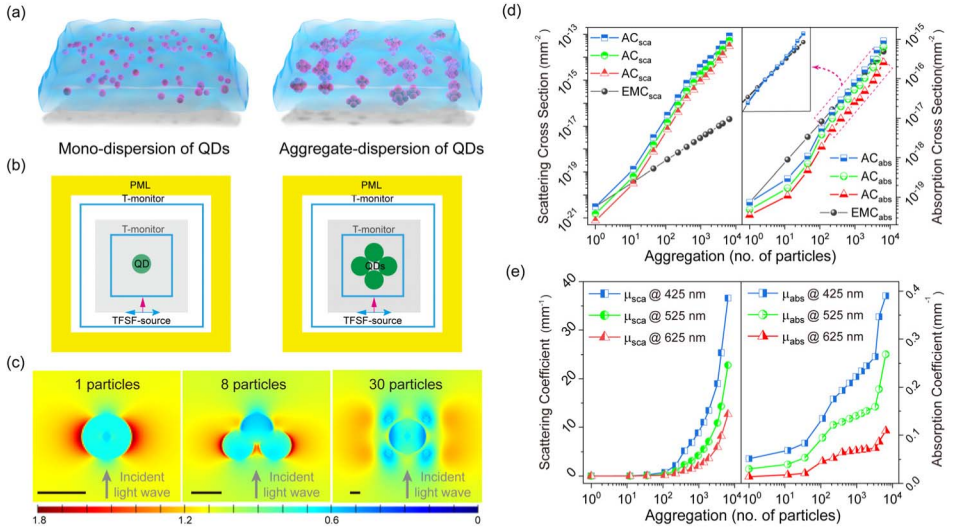

Fig. 2. (a) Diagram showing mono-dispersion (left) and aggregate-dispersion (right) systems for dispersing single QDs and QD-aggregates in a silicone matrix. (b) Diagram showing the FDTD setups for mono-dispersion (left) and aggregate-dispersion (right) systems. (c) Cross-sectional view of the electromagnetic field distributions produced by QDs having an aggregate size of 1 (mono-dispersion), 8, and 30 particles. Scale bar: 10 nm. (d) Scattering and absorption cross sections of the QDs as a function of the degree of aggregation. The inset shows a magnified potion of the absorption cross section curve corresponding to large aggregate sizes. (e) Scattering and absorption coefficients of the QD-silicone composites having a QD concentration of 0.8 wt%.

used to measure the electromagnetic energy distributions of the propagating light. Silicone was used as the background material for the free computational region having a refractive index of 1.41.

We used CdSe/ZnS QDs for our modeling, and their complex refractive index was set according to previous studies [31]. The size of a single QD was set to have a diameter of 10 nm according to the TEM images [see Fig. 1(d)]. A numerical mesh size of 0.05 nm was used to ensure accuracy of the simulations, and the simulation run time was set to be long enough to ensure energy convergence. Fig. 2(c) shows the resulting electromagnetic field distributions generated by the QDs having different degrees of aggregation, such as 1, 8, and 30 particles. We observe that the scattering energy is mainly concentrated along the edges of the QDs. This can be attributed to the diffraction effect caused by the refractive index difference between the QDs and silicone, particularly for the QD-aggregate having 30 particles. We further note that the energy distribution of a single QD is uniform, demonstrating less refracted incident light, whereas the energy distribution becomes more inhomogeneous as the degree of aggregation increases. Overall, these results indicate that larger QD-aggregates in silicone have a stronger scattering ability owing to their larger effective size, leading to the so-called AIS effect. A detailed quantitative study of this phenomenon has been carried out, which is discussed below.

Generally, the scattering cross section C_{sca} and the absorption cross section C_{abs} of particles can be calculated from the FDTD simulations. In the total-field region of the FDTD computational domain, both the incident and the scattered electromagnetic fields were included in the calculation, whereas in the scattered-field region, only the scattered electromagnetic field was included in the calculation. The total scattered power $P_{\text{sca}}(\lambda)$ and the total absorbed power $P_{\text{abs}}(\lambda)$ can be calculated according to the following equations:

$$P_{\text{sca}}(\lambda) = \sum_{i=1}^{n} T_i^{\text{scattered}}(\lambda) P(\lambda)$$

$$P_{\text{abs}}(\lambda) = \left(1 - \sum_{i=1}^{n} T_i^{\text{total}}(\lambda)\right) P(\lambda)$$

where $T_i^{\text{total}}(\lambda)$ and $T_i^{\text{scattered}}(\lambda)$ are the total and scattered transmissions, respectively, obtained from the series of monitors placed in the scattered field region; $P(\lambda)$ is the power of the incident source; and λ is the wavelength (nm).

Consequently, C_{sca} and C_{abs} can be calculated according to the following equations [32]:

$$C_{\text{abs}}(\lambda) = P_{\text{sca}}(\lambda)/I(\lambda)$$
$$C_{\text{abs}}(\lambda) = P_{\text{abs}}(\lambda)/I(\lambda)$$

where $I(\lambda)$ is the source irradiance (W/m^2). Similarly, the corresponding scattering cross section (AC_{sca}) and absorption cross section (AC_{abs}) of the QD-aggregates can be calculated from the scattered and absorbed powers obtained from aggregate-dispersion systems as discussed above. Note that a QD-aggregate actually constitutes of numerous single QD particles.

Thus, to compare various cross sections of a QD-aggregate in an aggregate-dispersion system with those of a single QD in a mono-dispersion system, the scattering and absorption cross sections of a single QD with equivalent degrees of aggregation are calculated according to the linear stacking method [33], [34]; in other words, it is a superposition of scattering and absorption cross sections in an ideal mono-dispersion system. Therefore, these are called the equivalent mono-dispersion scattering cross section (EMC_{sca}) and equivalent mono-dispersion absorption cross

section (EMC_{abs}), respectively. Fig. 2(d) shows the scattering and absorption cross sections of QD-aggregates (in aggregate-dispersion systems) and single QD particles (in mono-dispersion systems) as a function of the degree of aggregation. We used incident light from blue, green, and red sources, which correspond to wavelengths of 455, 525, and 625 nm, respectively, as these three colors are generally produced in QD displays. We observe that AC_{sca} increases as the degree of aggregation increases for all three wavelengths. Moreover, the AC_{sca} values are orders of magnitude larger than the corresponding EMC_{sca} values for the same degree of aggregation, particularly at large aggregate sizes. Therefore, it can be confirmed that the AIS effect in QD-aggregates is much stronger than the scattering effect caused by the linear superposition of single QDs in a mono-dispersion system even for the same degree of aggregation. These results can be attributed to the stronger intensity of AIS by QD-aggregates owing to their larger volume. We also note that the QD-aggregates demonstrate a stronger AIS effect on blue light compared with that on green and red lights, which is consistent with the Rayleigh scattering theory. Similarly, AC_{abs} increases with the degree of aggregation for all three wavelengths, and the absorption of blue light is stronger than that of green and red lights. It is interesting to note that the AC_{abs} values are smaller than the corresponding EMC_{abs} values for the same degree of aggregation at small aggregate sizes; however, the exact opposite trend is observed when the aggregate size reaches 1000 particles, as shown in the inset of Fig. 2(d). This is because the internal QDs in an aggregate with a close-packed structure have a lower absorption probability compared with the external QDs, thus leading to a smaller AC_{abs} compared with EMC_{abs} for the same degree of aggregation. Nevertheless, AC_{abs} exceeds EMC_{abs} as the degree of aggregation increases even more, which is attributed to the enhanced absorption loss caused by Rayleigh scattering in the QD-aggregates.

Furthermore, the scattering coefficient μ_{sca} and the absorption coefficient μ_{abs} are important parameters when investigating light propagation through a scattering medium, as they determine the scattering and absorption probabilities, respectively. It is assumed that individual QDs aggregate to form larger particles and these particles can then be uniformly dispersed in a silicone matrix to create QD-silicone composites; the exact degree of aggregation is neglected for convenience. In addition, multiple scattering events occur inside the particle cloud at low particle concentrations; however, the interparticle interactions can be neglected [34]. Therefore, the $P_{sca}(\lambda)$ and $P_{abs}(\lambda)$ values of the individual particles in a QD-aggregate can be added directly to obtain the total scattering and absorption powers of the QD-aggregate, respectively. Thus, the coefficients μ_{sca} and μ_{abs} of the QD-aggregate can be calculated using the following equations:

$$\mu_{sca}(\lambda) = N_i \frac{P_{sca}(\lambda)}{I(\lambda)} = \frac{c}{m} C_{sca}(\lambda)$$
$$\mu_{abs}(\lambda) = N_i \frac{P_{abs}(\lambda)}{I(\lambda)} = \frac{c}{m} C_{abs}(\lambda)$$

where N_i is the total number of particles per unit volume in the QD-aggregate ($1/m^3$); $P_{sca}(\lambda)$ and $P_{abs}(\lambda)$ are the scattering and absorption powers, respectively, of a single particle in the QD-aggregate; c is the particle concentration in the QD-aggregate (g/m^3); and m is the mass of a single particle in the QD-aggregate (g).

The scattering and absorption coefficients of the QD-aggregates as a function of their degree of aggregation are presented in Fig. 2(e). Herein, the QD concentration is kept at 0.8 wt%. Note that the QD-aggregate having only one particle corresponds to the case without aggregation, and its μ_{sca} and μ_{abs} can be calculated according to (7) and (8). We observe that the μ_{sca} curves for all three wavelengths coincide with each other for aggregate sizes of less than 100 particles, indicating a similar scattering ability in this regime. When the aggregate size reaches 1000 particles, μ_{sca} shows a significant increase with the degree of aggregation. Moreover, a higher concentration of particles in the QD-aggregates leads to a larger μ_{sca} for the same degree of aggregation. We also observe that μ_{sca} and μ_{abs} for red light are significantly smaller than those for blue and green lights. This implies that the red light experiences a smaller AIS effect, which further explains the reason behind the more widespread commercialization of red QD-devices. These results are consistent with the scattering cross section results [see Fig. 2(d)], both demonstrating a strong AIS effect in QD-silicone matrices having significant QD aggregation. In addition, the QD-aggregates still satisfy the Rayleigh scattering criteria owing to their overall small size. We have thus established the AIS model by evaluating the scattering ability of QD-aggregates, which provides a significant approach to investigate the AIS effects of QDs in silicone.

C. AIS Effect on the Efficiency of LED Devices

In order to have a convincing investigation of AIS effect on the efficiency of LED devices, the verification of AIS model has been carried out to determine the effective aggregate size (EAS) of QDs in silicone. First, we used the Monte Carlo RT method to investigate the AIS effect of QD-aggregates in silicone with various QD concentrations. Note that the RT method was used to carry out theoretical analysis for better comparing with the results of experiment. As shown in Fig. 3(a), the RT setup consisted of a QD-silicone composite with a diameter of 10 mm and a thickness of 0.5 mm, which had the same geometry as that used in the experiments (see Fig. 1); and a red laser source with a wavelength of 625 nm, which was incident perpendicular to the composite with an irradiated area of 0.126 mm^2. In addition, a semispherical detector with a radius of 1 m was placed behind the QD-silicone composite to record the transmitted power and NTID. The transmitted power of the QD-silicone composites with various QD concentrations is shown in Fig. 3(b). We observe that the transmitted power decreases significantly as the aggregation increases. For instance, the transmitted power decreases by 30% when the aggregate size reaches 1000 particles at a QD concentration of 0.8 wt%, and is reduced further as the aggregation keeps increasing. These results confirm that the

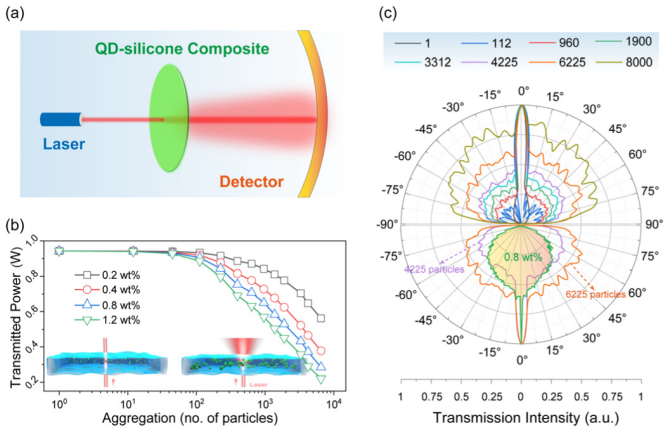

Fig. 3. (a) Schematic showing the laser system used in the RT method. (b) Transmitted power of the QD-silicone composites with different QD concentrations. The inserts show the laser propagation in silicone with mono-dispersion (left) and aggregate-dispersion (right) of QDs. (c) Simulated NTIDs for different aggregate sizes at a QD concentration of 0.8 wt% to determine the EAS via comparison method. The highlighted curve is the experimentally measured NTID for the QD-silicone composite with a concentration of 0.8 wt%.

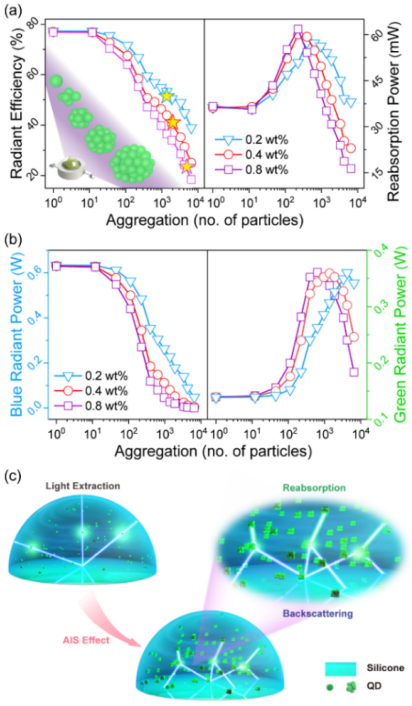

Fig. 4. (a) Radiant efficiency (left) and reabsorption power (right) of LED devices for various QD concentrations. The star symbols denote the efficiencies of the LED devices fabricated in this study with the QD concentrations of 0.2, 0.4, and 0.8 wt%. The inset shows the schematic of an LED device with a semispherical lens packaging structure. (b) Blue radiant power of LED chips (left) and green radiant power of QDs (right) for different QD concentrations. (c) Schematic demonstrating the AIS effect on LED devices.

AIS effect leads to serious backscattering in the QD-silicone composites. In general, higher QD concentrations result in lower transmitted powers for the same degree of aggregation, which can be explained by the higher with the larger number of QD-aggregates generated in this case. However, when the aggregate size is less than 50 particles, the transmitted power across different QD concentrations is almost constant, which is because of the weak scattering intensity at these aggregate sizes. In contrast, when the degree of aggregation is sufficiently high, the transmitted power decreases as the QD concentration increases. These results demonstrate that the large difference between the transmission spectra of the QD-silicone composites with different QD concentrations [see Fig. 1(b)] can be attributed to the more serious aggregation of QDs that occurs at higher concentrations.

As discussed above, the degree of aggregation can be larger at higher QD concentrations. In the following, we only consider the EAS of the QD particles for convenience, which is equivalent to the effective particle size of phosphors according to the Mie theory discussed in previous studies. First, from the RT model, we obtained the NTIDs of the QD-silicone composites having different degrees of aggregation for a specific QD concentration. These were subsequently used to determine the range for the EAS that best describes the QD-aggregates generated in the experiments. This is a reasonable approach because the NTID is mainly determined by the inner particles in the aggregate, where the film structure and concentration are roughly constant. Note that the schematic showing the laser propagation through the QD-silicone composite in the inserts of Fig. 3(b) intuitively demonstrates the NTID generated by the QD-aggregates. To obtain the EAS for the different QD composites, the QD concentration should be selected first, which determines the strength of the AIS effect. Subsequently, the EAS valid for the composites in the physical experiments can be obtained by comparing the experimental NTIDs with those obtained from the RT model. A QD concentration of 0.8 wt% was used as an example to compare the NTIDs based on the AIS model. As shown in Fig. 3(c), the NTID becomes more isotropic as the degree of aggregation increases, exhibiting the same trend as that obtained in the experiments [see Fig. 1(c)]. More importantly, we observe that the NTIDs generated by the RT model for the QD-silicone composites with an aggregate size ranging from 4225 to 6225 particles match very closely with the NTID obtained from the experiments at this QD concentration. The subtle difference in the NTIDs can be attributed to the fact that the laser system in real experiments is not an ideal collimating source and causes some light divergence. Based on this method, it can be obtained that the EAS for the QD-silicone composites in the experiments with a QD concentration of 0.8 wt% lies between 4225 and 6225 particles.

Furthermore, theoretical analysis with the AIS model have been performed to reveal the corresponding mechanisms on light-extraction for LED devices, and the results are presented in Fig. 4(a) and (b). In these cases, LED devices with a semispherical lens packaging structure were selected owing to their excellent light-extraction performance, as shown in the inset of Fig. 4(a). The radiant power of LED devices with various QD concentrations and degrees of aggregation was simulated using the RT method. Herein, the AIS effect on the light-extraction performance of LED devices, as well as the color-conversion process which contains the effect of

the reabsorption loss of QDs, are considered for developing a comprehensive simulation. We set the initial light extraction efficiency of blue-chip LEDs according to that of blank LED devices with an injection current of 50 mA and their color conversion efficiency was selected according to the PLQY of green QDs, so as to better compare with the fabricated devices. The left column of Fig. 4(a) presents the radiant efficiencies of the LED devices with various QD concentrations. It is observed that when there is no aggregation, the radiant efficiency remains almost constant even at a high QD concentration of 0.8 wt%; however, the efficiency decreases significantly as the aggregation increases for various QD concentrations. Note that the radiant efficiencies for all concentrations start to drop when the aggregate size reaches 50 particles, and decline sharply as the aggregation continues to increase. For instance, the radiant efficacy of the LED device drops by 22.3% for a QD concentration of 0.2 wt% as the aggregate size increases to 1000 particles, whereas the efficiency drops by 37.1% for a concentration of 0.8 wt%, compared with the corresponding cases without aggregation. This reduction in the radiant efficiency is more obvious at higher QD concentrations when the aggregation is more serious. The decreasing trend of efficiencies obtained by RT method is in agreement with the literatures [35], [36]. Furthermore, we also fabricated experimental LED devices with QD concentrations of 0.2, 0.4, and 0.8 wt% to verify the above results. The radiant efficiencies of these fabricated LED devices are denoted in Fig. 4(a) with stars. We observe that the radiant efficiency of the fabricated device with a QD concentration of 0.8 wt% is such that the corresponding QD-aggregate size indeed lies within the range of 4225–6525 particles, which is consistent with the EAS obtained using the RT method. This result validates the feasibility and accuracy of AIS model and further the EAS for different QD concentrations can be inferred using the same method, demonstrating a stronger AIS effect, which in turn implies that the QD-aggregates generated have a larger effective size.

In general, QDs exhibit a strong reabsorption of their emitted light, which is comparable with the excitation blue light from LED chips and leads to energy transfer process and serious reabsorption [37]. The reabsorption power of LED devices with different QD concentrations is calculated using the steady-iteration method, and the corresponding results are presented in the right column of Fig. 4(a). It is observed that the reabsorption power increases significantly as the degree of aggregation increases and reaches a peak once the aggregate size crosses hundreds of particles. In particular, devices with higher QD concentrations exhibit a more rapid increase in reabsorption power and also have a higher reabsorption peak. This is attributed to the fact that larger QD-aggregates in higher QD concentration have larger absorption cross sections, as shown in Fig. 2(d), which in turn leads to more serious reabsorption loss. However, the reabsorption power decreases when the aggregation continues to increase. Owing to the generation of larger QD-aggregates, the light emitted from chip cannot reaches the inner QDs and the color conversion only occurs on the surface of the QD-aggregates, thus reducing the reabsorption loss. We further conducted a spectral energy analysis to achieve a deeper understanding of the AIS effect, the results of which are presented in Fig. 4(b). We observe that the radiant power of the blue light emitted by the LED chips decreases with an increase in aggregation, whereas that of the green light emitted by the QDs first increases, then shows roll-off as aggregation further increases. The increase in the green radiant power is attributed to the strong scattering effect caused by the QD-aggregates, which enhances the color conversion by QDs. The mechanism of the enhancement is similar to the common method for increasing LED efficiency by incorporating scattering nanoparticles in previous studies. The scattering effect caused by particles enhances the utilization of blue light, thereby increasing the conversion of QDs. Interestingly, the green radiant power of the LED devices drops sharply as aggregation continues to increase, especially at high QD concentrations. This can be explained by the fact that the QD-aggregates form a barrier around the LED chip, such that most of the light emitted by the chip as well as the QDs is trapped instantly and backscattered to the substrate. Consequently, the probabilities of color conversion by the QDs decrease sharply when the aggregation of QDs is extremely severe.

Most of the previous studies on the modeling and design of QD-white-LEDs believe that the scattering effect of QDs on the efficiency of these devices can be neglected owing to their nanometer order size. However, our results clearly demonstrate that the scattering loss (backscattering and reabsorption) caused by the QDs is significantly enhanced as the aggregation increases. More importantly, modeling and designing QD-white-LEDs without considering the AIS effect may lead to undesirable performance and efficiency. Therefore, it would be advisable to reduce the AIS loss in such LED devices by using a low QD concentration and a long-wavelength light source. Although it is essential to manage the aggregation of QDs in LED devices to reduce the AIS effect, this issue has been barely studied in the context of the efficiency of these devices. Therefore, the present study not only presents an essential mechanism that explains the low efficiency of QD-white-LEDs but also provides a promising way to model these devices by taking the AIS effect into consideration. In addition, an easier and more efficient nondestructive testing the degree of aggregation demonstrated by QDs in a silicone matrix can be devised by further optimizing our model in the future.

IV. Conclusion

In this study, we experimentally and theoretically investigated the AIS effect of QDs in silicone and unraveled the origin of low efficiency for QD-white-LED devices. The AIS effect on the optical behavior of QDs in silicone is quantitatively investigated, demonstrating that the strong scattering effect is attributed to the generation of a large aggregation of QD particles. Three-dimensional FDTD and RT simulations are carried out to establish the AIS model for QDs and the results indicate that the AIS effect is stronger for higher QD concentrations and leads to a larger EAS, which is confirmed by comparing with the experimental results of QD-silicone

films. For instance, the EAS for the QD-silicone composites having a concentration of 0.8 wt% is found to lie between 4225 and 6225 particles. Furthermore, the AIS effect on the efficiency of LED devices can be experimentally and theoretically obtained and it can be found that the AIS effect causes a significant reduction in the radiant efficiencies of QD-white-LEDs when the EAS exceeds 50 particles, which is validated by fabricated devices. The radiant efficacy of the LED device drops by 37.1% for a QD concentration of 0.8 wt%, compared with the corresponding cases without aggregation. According to the spectral energy analysis, it is confirmed that a strong AIS effect at high QD concentration leads to severe backscattering and reabsorption loss, which further results in a low device efficiency. Moreover, this study is also important for nondestructive testing the degree of aggregation demonstrated by QDs in a silicone matrix and for precisely modeling QD-white-LEDs.

REFERENCES

[1] X. Dai *et al.*, "Solution-processed, high-performance light-emitting diodes based on quantum dots," *Nature*, vol. 515, no. 6, pp. 96–99, Nov. 2014.

[2] X. Dai, Y. Deng, X. Peng, and Y. Jin, "Quantum-dot light-emitting diodes for large-area displays: Towards the dawn of commercialization," *Adv. Mater.*, vol. 29, no. 14, Apr. 2017, Art. no. 1607022.

[3] Y. Jin and X. Gao, "Plasmonic fluorescent quantum dots," *Nature Nanotechnol.*, vol. 4, no. 9, pp. 571–576, Sep. 2009.

[4] A. J. Nozik, "Quantum dot solar cells," *Phys. E, Low-Dimensional Syst. Nanostruct.*, vol. 14, nos. 1–2, pp. 115–120, 2002.

[5] Q. Zeng *et al.*, "Polymer-passivated inorganic cesium lead mixed-halide perovskites for stable and efficient solar cells with high open-circuit voltage over 1.3 V," *Adv. Mater.*, vol. 30, no. 9, 2018, Art. no. 1705393.

[6] D. Qi, M. Fischbein, M. Drndić, and S. Šelmi'c, "Efficient polymer-nanocrystal quantum-dot photodetectors," *Appl. Phys. Lett.*, vol. 86, no. 9, Feb. 2005, Art. no. 093103.

[7] B. Yu, S. Liang, X. Ding, Z. Li, and Y. Tang, "A sandwich structure light-trapping fluorescence antenna with large field of view for visible light communication," *IEEE Trans. Electron Devices*, vol. 68, no. 2, pp. 565–571, Feb. 2021.

[8] Y. Shirasaki, G. J. Supran, M. G. Bawendi, and V. Bulović, "Emergence of colloidal quantum-dot light-emitting technologies," *Nature Photon.*, vol. 7, no. 1, p. 13, 2013.

[9] Z.-T. Li *et al.*, "Investigation of light-extraction mechanisms of multi-scale patterned arrays with rough morphology for GaN-based thin-film LEDs," *IEEE Access*, vol. 7, pp. 73890–73898, 2019.

[10] Z. Li *et al.*, "Highly efficient and water–stable lead halide perovskite quantum dots using superhydrophobic aerogel inorganic matrix for white light–emitting diodes," *Adv. Mater. Technol.*, vol. 5, no. 2, Feb. 2020, Art. no. 1900941.

[11] F. Meinardi *et al.*, "Large-area luminescent solar concentrators based on 'Stokes-shift-engineered' nanocrystals in a mass-polymerized PMMA matrix," *Nature Photon.*, vol. 8, no. 5, pp. 392–399, May 2014.

[12] H. Li, K. Wu, J. Lim, H.-J. Song, and V. I. Klimov, "Doctor-blade deposition of quantum dots onto standard window glass for low-loss large-area luminescent solar concentrators," *Nature Energy*, vol. 1, no. 12, pp. 1–9, Dec. 2016.

[13] B. Xie, R. Hu, and X. Luo, "Quantum dots-converted light-emitting diodes packaging for lighting and display: Status and perspectives," *J. Electron. Packag.*, vol. 138, no. 2, Jun. 2016.

[14] J.-S. Li, Y. Tang, Z.-T. Li, X.-R. Ding, L.-S. Rao, and B.-H. Yu, "Effect of quantum dot scattering and absorption on the optical performance of white light-emitting diodes," *IEEE Trans. Electron Devices*, vol. 65, no. 7, pp. 2877–2884, Jul. 2018.

[15] H. Y. Kim *et al.*, "Quantum dot/siloxane composite film exceptionally stable against oxidation under heat and moisture," *J. Amer. Chem. Soc.*, vol. 138, no. 50, pp. 16478–16485, Dec. 2016.

[16] B. Janjua *et al.*, "True yellow light-emitting diodes as phosphor for tunable color-rendering index laser-based white light," *ACS Photon.*, vol. 3, no. 11, pp. 2089–2095, Nov. 2016.

[17] X. Li *et al.*, "$CsPbX_3$ quantum dots for lighting and displays: Room-temperature synthesis, photoluminescence superiorities, underlying origins and white light-emitting diodes," *Adv. Funct. Mater.*, vol. 26, no. 15, pp. 2435–2445, 2016.

[18] X. Li, Y. Liu, X. Song, H. Wang, H. Gu, and H. Zeng, "Intercrossed carbon nanorings with pure surface states as low-cost and environment-friendly phosphors for white-light-emitting diodes," *Angew. Chem. Int. Ed.*, vol. 54, no. 6, pp. 1759–1764, Feb. 2015.

[19] A. B. Greytak *et al.*, "Alternating layer addition approach to CdSe/CdS core/shell quantum dots with near-unity quantum yield and high on-time fractions," *Chem. Sci.*, vol. 3, no. 6, pp. 2028–2034, 2012.

[20] H. Shen *et al.*, "Highly efficient blue–green quantum dot light-emitting diodes using stable low-cadmium quaternary-alloy ZnCdSSe/ZnS core/shell nanocrystals," *ACS Appl. Mater. Interfaces*, vol. 5, no. 10, pp. 4260–4265, May 2013.

[21] J.-S. Li, Y. Tang, Z.-T. Li, W.-Q. Kang, X.-R. Ding, and B.-H. Yu, "Study on reabsorption properties of quantum dot color convertors for light-emitting diode packaging," *J. Electron. Packag.*, vol. 141, no. 4, Dec. 2019, Art. no. 041006.

[22] S. Yu, Y. Tang, Z. Li, K. Chen, X. Ding, and B. Yu, "Enhanced optical and thermal performance of white light-emitting diodes with horizontally layered quantum dots phosphor nanocomposites," *Photon. Res.*, vol. 6, no. 2, pp. 90–98, 2018.

[23] S. Mathew *et al.*, "Size dependent optical properties of the CdSe-CdS core-shell quantum dots in the strong confinement regime," *J. Appl. Phys.*, vol. 111, no. 7, Apr. 2012, Art. no. 074312.

[24] Y. Narukawa, M. Ichikawa, D. Sanga, M. Sano, and T. Mukai, "White light emitting diodes with super-high luminous efficacy," *J. Phys. D, Appl. Phys.*, vol. 43, no. 35, Sep. 2010, Art. no. 354002.

[25] J.-S. Li *et al.*, "Toward 200 lumens per watt of quantum-dot White-Light-Emitting diodes by reducing reabsorption loss," *ACS Nano*, vol. 15, no. 1, pp. 550–562, Jan. 2021.

[26] H. Zhang, Q. Su, Y. Sun, and S. Chen, "Efficient and color stable white quantum-dot light-emitting diodes with external quantum efficiency over 23%," *Adv. Opt. Mater.*, vol. 6, no. 16, Aug. 2018, Art. no. 1800354.

[27] Y. Tang, Z. Li, G. Liang, Z. Li, J. Li, and B. Yu, "Enhancement of luminous efficacy for LED lamps by introducing polyacrylonitrile electrospinning nanofiber film," *Opt. Exp.*, vol. 26, no. 21, pp. 27716–27725, 2018.

[28] S. Yu *et al.*, "Enhanced photoluminescence in quantum dots–porous polymer hybrid films fabricated by microcellular foaming," *Adv. Opt. Mater.*, vol. 7, no. 12, Jun. 2019, Art. no. 1900223.

[29] W. Hergert and T. Wriedt, *The Mie Theory: Basics and Applications*, vol. 169. Springer, 2012.

[30] K. Yee, "Numerical solution of initial boundary value problems involving Maxwell's equations in isotropic media," *IEEE Trans. Antennas Propag.*, vol. AP-14, no. 3, pp. 302–307, May 1966.

[31] J. Lee, K. Min, Y. Park, K. Cho, and H. Jeon, "Photonic crystal phosphors integrated on a blue LED chip for efficient white light generation," *Adv. Mater.*, vol. 30, no. 3, Jan. 2018, Art. no. 1703506.

[32] A. R. Jones, "Light scattering for particle characterization," *Prog. Energ. Combustion Sci.*, vol. 25, no. 1, pp. 1–53, 1999.

[33] S. A. Prahl, "A Monte Carlo model of light propagation in tissue," *Proc. SPIE*, vol. 1035, Jan. 1989, Art. no. 1030509.

[34] J.-S. Li *et al.*, "A detailed study on phosphor-converted light-emitting diodes with multi-phosphor configuration using the finite-difference time-domain and ray-tracing methods," *IEEE J. Quantum Electron.*, vol. 51, no. 10, pp. 1–10, Oct. 2015.

[35] S. Jun, J. Lee, and E. Jang, "Highly luminescent and photostable quantum Dot–Silica monolith and its application to light-emitting diodes," *ACS Nano*, vol. 7, no. 2, pp. 1472–1477, Feb. 2013.

[36] Z.-T. Li, J.-X. Li, J.-S. Li, Z.-H. Deng, Y.-H. Deng, and Y. Tang, "Scattering effect on optical performance of quantum dot white light-emitting diodes incorporating SiO_2 nanoparticles," *IEEE J. Quantum Electron.*, vol. 56, no. 3, Jun. 2020, Art. no. 3600109.

[37] J. Chen *et al.*, "Efficient and bright white light-emitting diodes based on single-layer heterophase halide perovskites," *Nature Photon.*, pp. 1–7, 2020.